

1 **Using genomic epidemiology and geographic activity spaces to investigate tuberculosis**
2 **outbreaks in Botswana**

3

4 **Chelsea R. Baker, Ivan Barilar, Leonardo S. de Araujo, Daniel M. Parker, Kimberly**
5 **Fornace, Patrick K. Moonan, John E. Oeltmann, James L. Tobias, Volodymyr M. Minin,**
6 **Chawangwa Modongo, Nicola M. Zetola¹, Stefan Niemann¹, and Sanghyuk S. Shin¹**

7 Author affiliations: University of California, Irvine, California, USA (C.R. Baker, D.M. Parker,
8 V.M. Minin, S.S. Shin); Forschungszentrum, Borstel, Germany (I. Barilar, L.S. de Araujo, S.
9 Niemann); National University of Singapore (K. Fornace); US Centers for Disease Control and
10 Prevention, Atlanta, Georgia, USA (P.K. Moonan, J.E. Oeltmann, J.L. Tobias,); Botswana–
11 Upenn Partnership, Gaborone, Botswana/ Victus Global Botswana Organisation, Gaborone,
12 Botswana (C. Modongo, N.M. Zetola)

13

14 ¹These senior authors contributed equally to this article.

15 **Corresponding author:**

16 Sanghyuk Shin, PhD

17 Associate Professor, Sue & Bill Gross School of Nursing

18 Email: ssshin2@uci.edu

19 Phone: 949-576-8675

20

21 **Key words:** Tuberculosis transmission, spatial analysis, activity space, whole genome

22 sequencing, geographic heterogeneity, outbreak, infectious disease control

23 **Abstract**

24 Background

25 The integration of genomic and geospatial data into infectious disease transmission analyses
26 typically includes residential locations and excludes other activity spaces where transmission
27 may occur (*e.g.* work, school, or social venues). The objective of this analysis was to explore
28 residential as well as other activity spaces of tuberculosis (TB) outbreaks to identify potential
29 geospatial ‘hotspots’ of transmission.

30 Methods

31 We analyzed data that included geospatial coordinates for residence and other activity spaces
32 collected during 2012–2016 for the Kopanyo Study, a population-based study of TB transmission
33 in Botswana. We included participants with results from whole genome sequencing conducted on
34 archived samples from the original study. We used a spatial log-Gaussian Cox process model to
35 detect core areas of increased activity spaces of individuals belonging to TB outbreaks
36 (genotypic groups with ≤ 5 single-nucleotide polymorphisms), which we compared to ungrouped
37 participants (those not in a genotypic group of any size).

38 Findings

39 We analyzed data collected from 636 participants, including 70 participants belonging to six
40 outbreak groups with a combined total of 293 locations, and 566 ungrouped participants with a
41 combined total of 2289 locations. Core areas of activity space for each outbreak group were
42 geographically distinct, and we found evidence of localized transmission in four of six outbreaks.
43 For most of the outbreaks, including activity space data led to the detection of larger areas of
44 higher spatial intensity and more focal points compared to residential location alone.

45 Interpretation

46 Geospatial analysis using activity space data (social gathering places as well as residence) may
47 lead to improved understanding of areas of infectious disease transmission compared to using
48 residential data alone.

49 Funding

50 This work was supported by funding from the National Institute of Allergy and Infectious
51 Diseases R01AI097045, R01AI147336, and R01AI170204.

52

53 **Background**

54 Tuberculosis (TB) remains among the leading causes of death due to infectious illness, despite
55 being a preventable and curable disease¹. In 2022, over 10 million people became sick with TB,
56 and 1.3 million died¹. Progress toward TB elimination has been slow and many targets set by the
57 World Health Organization (WHO) have not been met¹. New strategies and tools are needed for
58 TB prevention¹. In high-burden settings, where a substantial portion of disease incidence is due
59 to recent infection, interventions to stop ongoing transmission are especially important¹⁻⁵.

60
61 A promising tool is the integration of geospatial and pathogen genomic data. Pathogen whole
62 genome sequencing (WGS) can be used to identify closely related *M. tuberculosis* isolates and
63 help reconstruct likely transmission chains⁶. Geographic and genomic data can be combined to
64 help detect areas of sustained transmission, locate outbreaks, and investigate the geographic
65 range of different strains^{7,8}. Spatial analysis of WGS data can help identify high-risk areas that
66 could be targeted for public health interventions to interrupt ongoing transmission^{3-7,9-15}.

67 Geographically targeted interventions have shown promise as an effective and cost-efficient
68 strategy for reducing TB incidence in high-burden, low-resource settings¹⁶⁻¹⁹.

69
70 However, an important limitation to many studies employing this strategy is geospatial analysis
71 based solely on residential location, which excludes locations in the community where
72 transmission may occur^{12,20-22}. An alternative approach is to analyze “activity space,” which
73 includes the places one routinely occupies during day to day life²³⁻²⁵. For example, this may
74 include residential as well as community sites such as workplaces, markets, places of worship, or

75 other social gathering places^{23,24}. This approach has the potential to lead to more accurate
76 detection of high-risk areas compared to analysis of residential locations alone^{24,26}.

77

78 We previously conducted a descriptive study of geospatial residential data and WGS data from a
79 population-based study of TB transmission in Botswana found evidence that TB outbreaks
80 displayed distinct geographic characteristics²⁷. The objectives of the current analysis were to use
81 spatial statistical modeling to 1) identify geographic characteristics of the collective activity
82 space (residential as well as social gathering locations) of each outbreak group, and 2) identify
83 potential ‘hotspot’ areas of activity space associated with each outbreak, which may represent
84 areas of increased risk for transmission.

85

86 **Methods**

87 Study design and setting

88 We analyzed data collected during 2012–2016 for the Kopanyo Study, a population-based study
89 of TB transmission in Botswana, a country in southern Africa with a high burden of TB and
90 TB/HIV co-infection^{1,5,28}. Participants were recruited at multiple local health clinics in two
91 districts: Gaborone, the urban center and capital city, and Ghanzi, a rural district several hundred
92 kilometers away^{5,28}. During the five years before the study, TB incidence was 440–470
93 cases/100,000 persons in Gaborone, which had a total population of 354,380, and 722
94 cases/100,000 persons in Ghanzi, which had a population of 44,100 (12,179 in Ghanzi town)^{5,28}.

95

96 Study participants included men and women of all ages with TB disease who were sequentially
97 enrolled by date of diagnosis^{5,28}. Those who had already received TB treatment for >14 days,

98 prisoners, and patients who declined to participate were excluded^{5,28}. At least 1 sputum sample
99 was collected from each participant for bacterial culture^{5,28}. Clinical and demographic data were
100 collected through in-person interviews and medical record review^{5,28}.

101
102 Data gathered during participant intake interviews included high resolution geospatial data for
103 activity space, which included home residence and social gathering places^{5,28}. Participants were
104 asked about residential location as well as social gathering places (e.g. workplaces, schools,
105 markets, places of worship, alcohol venues etc.) frequented during their potential infectious
106 period (up to 12 months prior to treatment initiation)^{5,28}. Geographic coordinates (latitude and
107 longitude recorded using the WGS 84 projection system with 1.1-m precision) for locations were
108 obtained using global positioning system (GPS) devices during site visits, or by geocoding
109 addresses using a reference layer created by manually relocating addresses in satellite imagery
110 using Google Maps, OpenStreetMap, and ArcGIS^{5,28}.

111

112 WGS

113 Whole genome sequencing was conducted on DNA samples archived from the original study
114 with sufficient quantities of DNA (>0.05 ng/ μ L) for analysis. Closely related *M. tuberculosis*
115 isolates were identified bioinformatically using a single linkage clustering algorithm. We
116 considered clusters of isolates with ≤ 5 single-nucleotide polymorphisms (SNPs) to indicate
117 recent transmission and clusters of ≥ 10 persons to be outbreaks. Further details of this procedure
118 are outlined in a separate analysis²⁷.

119

120 Spatial modeling of activity space

121 Participants eligible for the current analysis included those with WGS data, GPS coordinates,
122 and sociodemographic data for age, sex, income, and HIV status available. We focused our
123 current analysis on outbreak groups that had at least 10 activity space locations (collectively
124 among all their participants) within greater Gaborone, an area of approximately 27 km x 24 km
125 that includes the capital city and its surrounding suburbs. We also included genotypically
126 ungrouped participants as a comparison group. For model fitting purposes, a very small jitter was
127 introduced to location coordinates to avoid duplicate points (roughly on the scale of different
128 areas of the same building, ranging from approximately <1 to 10 meters).

129
130 We conducted a preliminary analysis to compare the geographic distribution of participants with
131 WGS data available to the total study population from the Kopanyo Study to rule out geographic
132 sampling bias. We estimated the geographic median center (a centralized point that minimizes
133 the distance to all other points), and directional distribution (which calculates the standard
134 deviation of points along both the X and Y axes) for both groups of participants and found nearly
135 identical results, indicating that participants with WGS data were geographically representative
136 of the larger study population. This analysis was performed using ArcGIS²⁹.

137

138 Model description

139 We used a spatial log-Gaussian Cox process (LGCP) to model the spatial intensity (average
140 number of points per unit area) of activity spaces of participants belonging to each outbreak
141 group ('cases') and of genotypically ungrouped participants (those not in an identified genotypic
142 group of any size, 'controls'). LGCPs are a flexible class of models for spatial point processes
143 where spatial intensity may vary across the study region^{30,31}. A spatial random effect can be

144 incorporated to account for spatial correlation in the data and identify spatial patterns not
145 explained by other variables^{33,34,37,40}. This technique offers a model-based approach for
146 estimating utilization distributions, which are probability density functions that can be mapped to
147 highlight areas with increased geographic concentrations of points (e.g. activity space locations)
148 to help characterize use of space^{26,32}. To adapt the modeling framework to an activity space
149 context where each individual may be associated with multiple point locations, observations can
150 be treated as cumulative ‘encounters’ over specified time periods³². We considered each point to
151 represent an ‘encounter’ in space corresponding to a potential TB exposure, and estimated
152 intensity surfaces for cumulative exposures over the entire study period.

153
154 LGCPs fit well in a Bayesian hierarchical modeling framework, and various tools can be used for
155 this approach^{33–35}. We used integrated nested Laplace approximation (INLA), a flexible and
156 computationally efficient method for approximate Bayesian inference for latent Gaussian
157 models, which include LGCPs^{33,34,36–38}. We implemented this using the R-INLA package³⁹. We
158 modeled the spatial random effect as a Gaussian random field (GRF) with Matérn
159 covariance^{37,38,40}. We used the stochastic partial differential equation (SPDE) approach in R-
160 INLA to approximate the GRF^{37,38,40}. We specified the SPDE model using penalized complexity
161 priors that were vaguely informative about the underlying spatial process (prior probability of
162 0.05 that the ranges of the fields were less than 0.5 km and prior probability of 0.05 that the
163 standard deviation was greater than 10).

164
165 Under the LGCP framework, we used a joint modeling approach to incorporate a shared spatial
166 term (obtained by jointly estimating the intensity of both cases and controls), as well as a unique

167 spatial term estimated for cases in each group^{38,41}. Using this approach, posterior mean estimates
168 of the spatial random effect for cases represent variation in intensity not accounted for by the
169 spatial distribution of controls⁴¹. We did this to help identify areas with relatively high
170 concentrations of activity spaces associated with individual outbreak groups, while attempting to
171 account for baseline use of space (as some locations tend to be frequented by people more often
172 in general). Areas with a high density of activity spaces frequented by people belonging to the
173 same outbreak group could potentially represent areas associated with an increased risk of recent
174 transmission. We fit a version of the model that included just the shared spatial term (model 0),
175 and a version of the model that included the shared spatial term as well as unique spatial terms
176 estimated for each outbreak group individually (model 1). We also conducted a sensitivity
177 analysis using subsets of the data with 70 and 140 randomly selected ungrouped participants as
178 controls to examine whether spatial patterns were sensitive to size of the control group.

179

180 We projected posterior mean estimates of the spatial effect (i.e. the effect of spatial location on
181 the intensity of activity spaces, represented by the spatial random field) for each outbreak group
182 onto maps of the study area in order to visualize how it varied across the region, and to identify
183 areas of increased or decreased (different than zero) values not explained by the spatial
184 distribution of controls⁴¹. Estimated values (displayed on the internal linear predictor scale)
185 represent the contribution of the spatial random effect to the response (spatial intensity) after
186 accounting for other fixed and random effects in the model. In addition, we reported posterior
187 mean estimates for the range (distance at which spatial correlation falls close to zero) and
188 variance of the spatial effect for each outbreak group³⁶.

189

190 We also projected posterior mean estimates for predicted spatial intensity values (fitted values of
191 the response at prediction locations, obtained by exponentiating the linear predictor), in order to
192 visualize patterns of spatial intensity of activity spaces for each outbreak group^{36,38}.

193

194 In addition, we calculated exceedance probabilities and projected these onto maps of the study
195 area to identify areas where estimated spatial effect for each outbreak group had a high
196 probability (0.95) of being greater than zero, representing high-confidence areas where the
197 spatial effect for cases was above the baseline that could be accounted for by the spatial
198 distribution of controls⁴¹. We also calculated exceedance probabilities to identify high-
199 confidence areas where the estimated spatial intensity was in the top ten percent of estimated
200 mean values for each group, representing 'core areas' or 'hotspots' of that group's collective
201 activity space³².

202

203 We also generated exceedance probability maps based only on location of participant residence
204 (using the same threshold values as the full analysis) to compare high-risk areas identified using
205 activity space analysis vs. home location alone. We projected these exceedance probabilities onto
206 interactive maps of the study area for each outbreak group.

207

208 Map visualization was performed using the R packages raster, terra, sf, ggplot2, ggspatial, and
209 leaflet.

210

211 **Results**

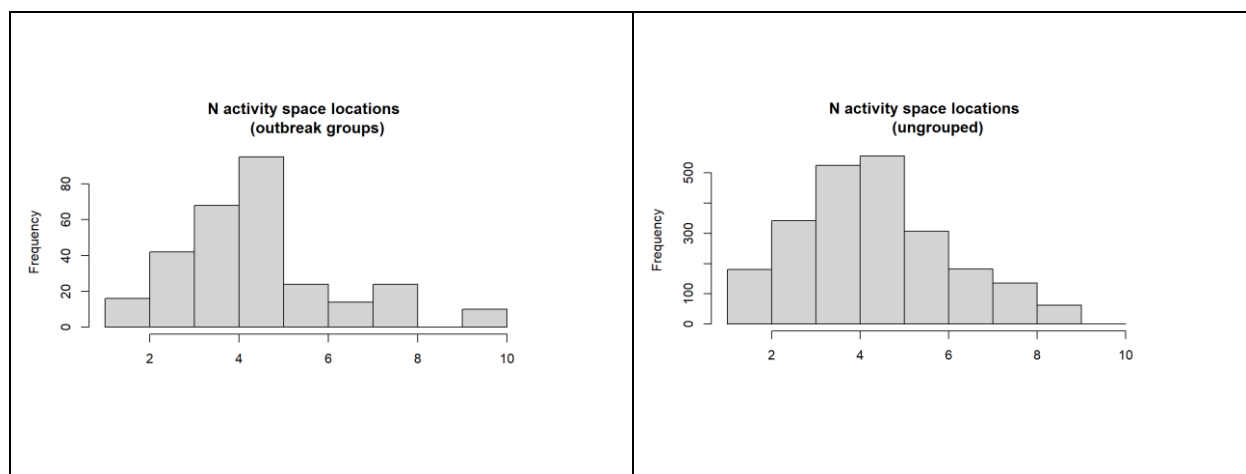
212 Participants

213 A total of 1426 participants had WGS data available, of which 1425 had GPS coordinates
214 available for at least one activity space location (home or social gathering place). Participants
215 with and without WGS data had similar sociodemographic characteristics in terms of age, sex,
216 HIV status, and income. Eight genotypic groups had 10 participants or more and were considered
217 outbreaks. Six out of eight outbreaks (genotypic groups with 10 participants or more) had at least
218 10 activity spaces (collectively among all their participants) in greater Gaborone.

219 A total of 636 participants with activity spaces in greater Gaborone met criteria for the current
220 analysis, including 70 participants belonging to six outbreak groups with a combined total of 293
221 locations, and 566 ungrouped participants with a combined total of 2289 locations.

222
223 Each participant had between one and 10 activity space locations, and the median number of
224 locations (n=4) was the same for both grouped and ungrouped participants (Figure 1). Median
225 number of activity space locations was the same (n=4) by gender and HIV status, though was
226 slightly lower for participants with no income (n=3) than participants with any income (n=4),
227 which could reflect an increased number of activity spaces among participants who were
228 employed. Among participants with more than one location, the maximum distance between any
229 two of their activity spaces ranged from <0.5 km to 21.2 km (median 6.2 km) for ungrouped
230 participants and <0.5 km to 21.7 km (median 4.3 km) for participants in outbreak groups
231 (supplementary figure 1).

232
233 Figure 1. Histograms for distribution of number of activity space locations per participants for
234 outbreak and genotypically ungrouped participants.



235

236 Among genotypically ungrouped participants, the median age was 35 years (IQR: 28–42), just
 237 over half were male, about one quarter reported no income, and nearly 65% were diagnosed with
 238 TB-HIV coinfection (Table 1). Among participants in the six genotypic groups, median age
 239 ranged from 30 years (Group A) to 39 years (Group G) (Table 1). Participants in Group G were
 240 exclusively male, while Group C alone was majority female (75%). Group D had the highest
 241 proportion of participants diagnosed with TB-HIV coinfection (9 of 11; 91%). The percentage of
 242 participants reporting no income ranged from 18% in Group D to 58% in Groups C and E (Table
 243 1).

244

245 Table 1. Characteristics of study participants (N = 636) by outbreak group (genotypic group \leq 5
 246 SNP), Gaborone, Botswana, 2012-2016

	A (N=22)	C (N=12)	D (N=11)	E (N=12)	G (N=9)	H (N=4)	Ungrouped (N=566)
Total locations	81	45	53	54	44	16	2289
Gender							

	A (N=22)	C (N=12)	D (N=11)	E (N=12)	G (N=9)	H (N=4)	Ungrouped (N=566)
Female	11 (50.0%)	9 (75.0%)	5 (45.5%)	3 (25.0%)	0 (0%)	2 (50.0%)	264 (46.6%)
Male	11 (50.0%)	3 (25.0%)	6 (54.5%)	9 (75.0%)	9 (100%)	2 (50.0%)	302 (53.4%)
Age							
Median	29	31	33	35	39	24	35
[Q1,Q3]	[24, 37]	[29, 36]	[31, 42]	[29, 40]	[35, 42]	[20, 38]	[28, 42]
HIV Status							
Neg	10 (45.5%)	5 (41.7%)	1 (9.1%)	6 (50.0%)	4 (44.4%)	3 (75.0%)	203 (35.9%)
Pos	12 (54.5%)	7 (58.3%)	10 (90.9%)	6 (50.0%)	5 (55.6%)	1 (25.0%)	363 (64.1%)
Income							
Any	16 (72.7%)	5 (41.7%)	9 (81.8%)	5 (41.7%)	7 (77.8%)	2 (50.0%)	417 (73.7%)
None	6 (27.3%)	7 (58.3%)	2 (18.2%)	7 (58.3%)	2 (22.2%)	2 (50.0%)	149 (26.3%)

247

248 Estimated spatial effects

249 Model 1 (shared and group-specific spatial terms) had a lower DIC (-12956.58) than model 0
 250 (shared spatial terms only, DIC -12853.84), supporting the presence of spatial variation among
 251 genotypic groups not accounted for by the spatial distribution of activity spaces of controls⁴¹.

252

253 In general, posterior estimates for the range of the spatial effects suggested small to medium
 254 scale spatial correlation (Table 2; Figure 2). The range was smallest for groups A and H,
 255 indicating that spatial correlation among points died off at relatively short distances. Both the
 256 range and variance were largest for group C, indicating the spatial effect spanned a greater

257 distance but also displayed ‘peaks’. This could be due to the presence of two distinct areas of
258 increased intensity located relatively far from one another.

259

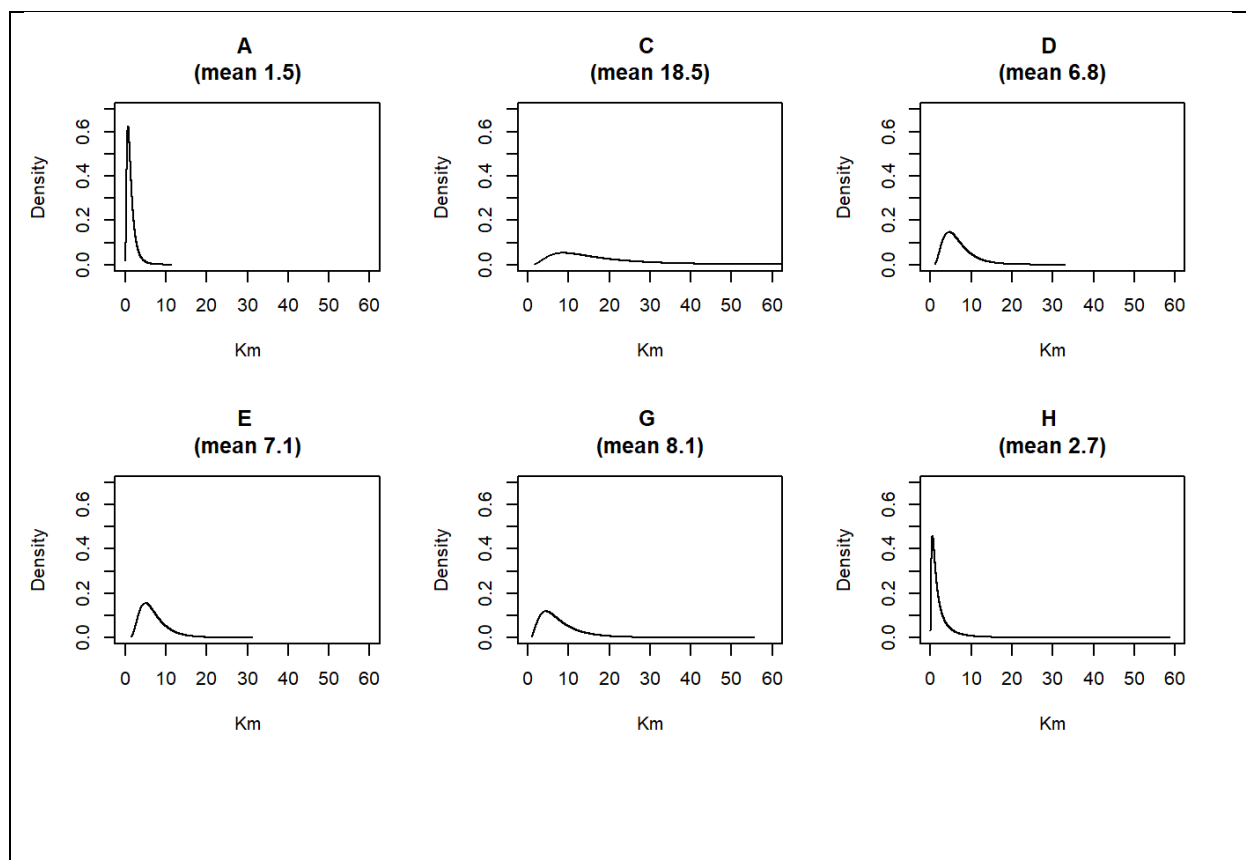
260 Table 2. Posterior mean estimates of the range and variance of the spatial effect for each outbreak
261 group (A-H), Gaborone, Botswana, 2012-2016.

	A	C	D	E	G	H
Range	1.5	18.5	6.8	7.1	8.1	2.7
(mean)						
Variance	0.1	2.0	0.6	1.4	1.8	0.5
(mean)						

262

263 Figure 2. Posterior mean estimates and marginal distributions of the range and variance of the
264 estimated spatial effect for each outbreak group, Gaborone, Botswana, 2012-2016

Posterior mean and marginal distribution for range for spatial effect (outbreak groups A – H)



265

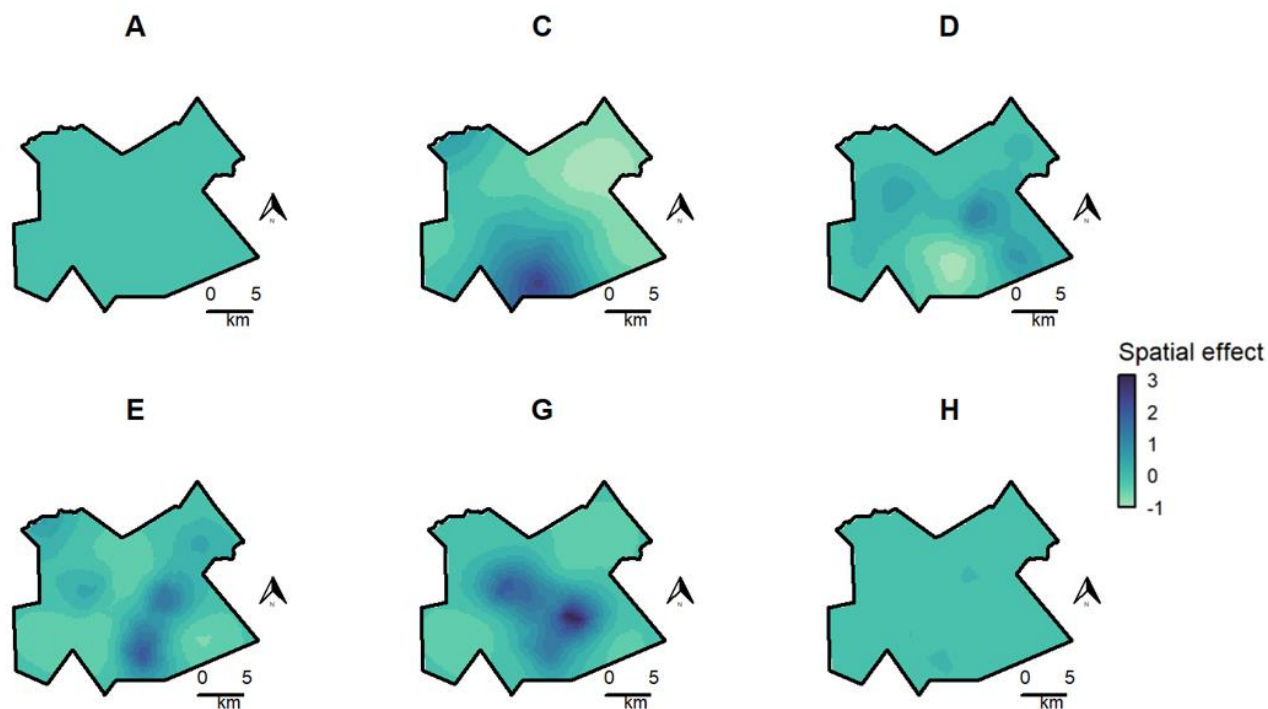
266 Maps of posterior mean estimates of spatial effects displayed different spatial patterns for each
267 outbreak group (Figure 3). Estimated spatial effects for group A and group H showed several
268 relatively small and dispersed areas of increased values compared to controls. Group C had a
269 notable area of increased spatial effect in the central southern part of the study area. Group D and
270 group G had two to three main areas of increased values that followed a broad east-west spread,
271 while for group E areas of increased estimates had a general north-south configuration.

272

273 Results of the sensitivity analysis using subsets of 70 and 140 randomly selected controls found
274 very similar results in terms of the spatial patterns and magnitude of estimated spatial effect by
275 group (Supplementary Figure 2 and Supplementary Figure 4).

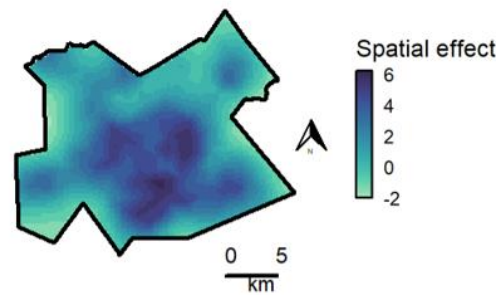
276

277 Figure 3. Posterior mean estimates of spatial random effect for each outbreak group (A-H) and
278 controls (ungrouped participants), Gaborone, Botswana, 2012-2016. Values are shown on the
279 internal linear predictor scale and represent the contribution of the spatial random effect on the
280 response, after accounting for other fixed and random effects in the model. Departures from
281 baseline (above or below zero) for outbreak groups measure group-specific spatial patterns that
282 are not accounted for by the spatial distribution of activity spaces of controls. Darker colors
283 correspond to increased spatial effect estimates. Values are displayed on the same color scale for
284 all outbreak groups, though on a separate color scale for controls due to difference in sample
285 size.
286



287

Ungrouped



288

289

290 Predicted spatial intensity

291 Maps of predicted mean spatial intensity displayed unique spatial patterns for each outbreak
292 group (Figure 4).

293

294 For group A, areas of increased spatial intensity of activity spaces followed an overall similar
295 pattern as seen for controls, with areas of highest intensity toward the center of the study area.

296 Group C had a distinct area of high intensity in the central southern part of the study area. Group

297 D had a notable area of increased intensity in the central east part of the map. Areas of highest

298 intensity for group E were in the central and south east, and for group G in the central east. The

299 areas of highest intensity for group H were located toward the center of the study area and also

300 resembled the overall spatial pattern seen for controls, though predicted values were relatively

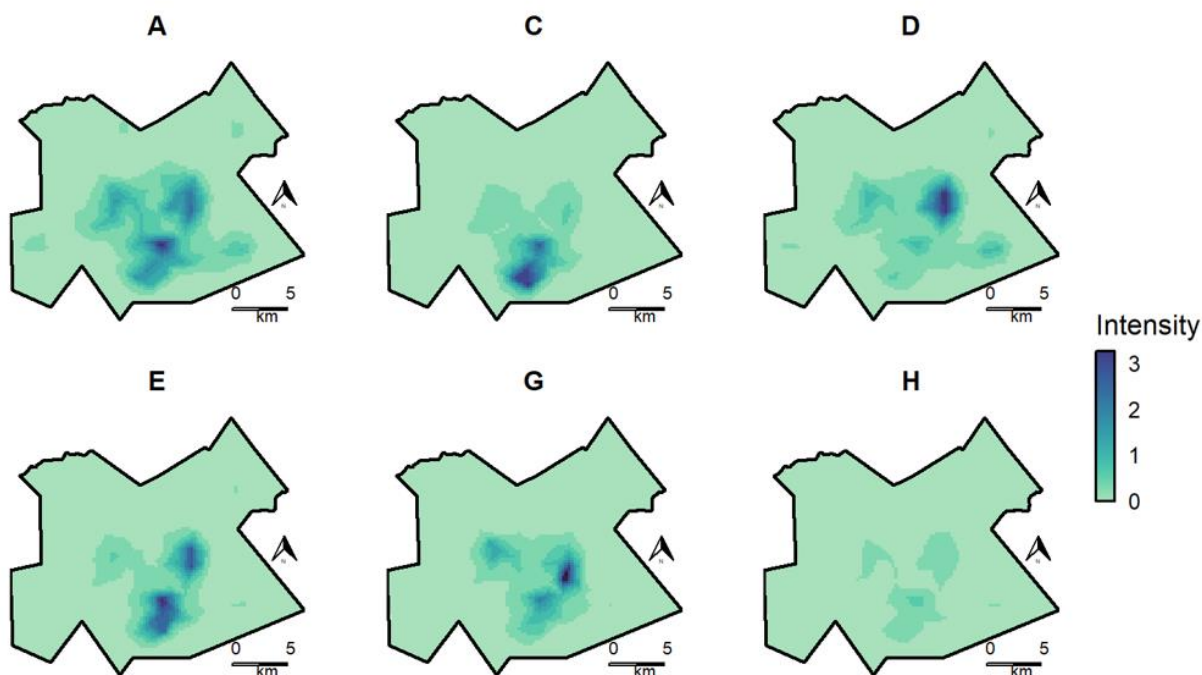
301 small compared to the other groups and not easily visible when mapped on the same color scale.

302

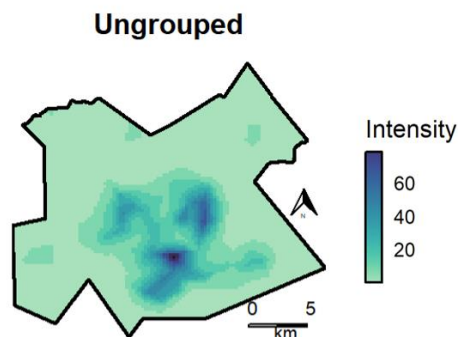
303 Results of the sensitivity analysis using subsets of 70 and 140 randomly selected controls found
304 very similar results for predicted spatial intensity by outbreak group (Supplementary Figure 3
305 and Supplementary Figure 5).

306

307 Figure 4. Predicted mean spatial intensity of activity spaces for participants in each outbreak
308 group (A-H) and controls (ungrouped participants), Gaborone, Botswana, 2012-2016. Values are
309 displayed on the response scale (obtained by exponentiating the linear predictor) and represent
310 predicted numbers of activity spaces per unit area (approximately 0.25 x 0.25 km). Areas of
311 increased intensity correspond to higher geographic concentration of activity spaces for
312 participants in each group. Intensity values are displayed on the same color scale for all outbreak
313 groups for ease of visual comparison, though on a separate color scale for controls due to
314 difference in sample size.



315



316

317

318 Exceedance maps

319 Exceedance maps for estimated spatial effects showed areas where the posterior mean had a high
320 probability (0.95) of being above 0 (greater than baseline) (Figure 5). Areas of significantly
321 increased spatial effect estimates based on full activity space analysis were detected for groups
322 C, D, E, and G. Groups A and H did not have areas meeting the specified threshold, which may
323 be due to a spatial distribution of activity spaces that resembles that of the control group.

324

325 Areas of significantly increased spatial effect estimates based on residential location alone were
326 detected for groups C and E, though not for groups A, D, G, or H. For group E, exceedance areas
327 based on activity space were geographically broader than those based solely on residential
328 location. For group C, exceedance areas were similar in both analyses.

329

330 Figure 5: Exceedance maps for spatial effect greater than 0 (departure above baseline) with high
331 probability (0.95) – full activity space and residential locations only, Gaborone, Botswana, 2012-
332 2016.

5.1 Full activity space



5.2 Residential only



333

334 Exceedance maps for predicted spatial intensity values showed distinct areas of high spatial
335 intensity ('core areas') for each outbreak group, corresponding to areas where posterior mean
336 intensity values had a high probability (0.95) of being in the upper ten percent of estimates for
337 that group (Figure 6).

338

339 In general, core areas based on residential location alone were geographically restricted
340 compared to core areas based on full activity space analysis. For all groups core areas based on
341 full activity space analysis were larger than those based on residential locations alone. For groups
342 A, D, G, and H, core areas based on activity space also involved additional geographic focal
343 areas-

344

345 Figure 6. Exceedance maps for predicted spatial intensity to display ‘core areas’ by outbreak
346 group based on full activity space and residential locations only, Gaborone, Botswana, 2012-
347 2016

6.1 Full activity space



6.2 Residential only



348

349 Discussion

350 In our analysis, we detected geographically distinct patterns of activity space associated with
351 different TB outbreak groups. Core areas ('hotspots') of highest spatial concentration of activity
352 spaces for each group were located in different areas, with some being more geographically
353 widespread and others more compact. For outbreak groups C, D, E, and G, we detected areas
354 where the spatial concentration of activity spaces of grouped participants was significantly
355 higher than the baseline spatial distribution of activity spaces of ungrouped controls (increased
356 spatial effect). This could suggest that distinct areas of localized transmission play an important

357 role in these outbreaks. The spatial distribution of activity spaces for groups A (the largest
358 outbreak group) and H (the smallest) resembled the overall spatial distribution of activity spaces
359 belonging to the control group. The differences in spatial characteristics among the groups could
360 potentially correspond to the timing of how long a genotype of TB has been circulating in the
361 community. It could also represent transmission among socially or geographically distinct
362 contact networks.

363

364 Activity space hotspots could represent potential high-priority areas for spatially targeted
365 interventions such as active case finding for TB and other infectious diseases. This may be
366 particularly useful for outbreaks involving localized transmission. Exceedance maps displaying
367 core areas of spatial intensity and areas of increased spatial effects such as those shown above
368 could potentially be a useful tool for public health planning. We displayed static snapshots from
369 interactive maps at a relatively low spatial resolution to protect privacy, though in practice such
370 maps could be used to examine potential hotspots at different spatial scales.

371

372 We also found differences between exceedance areas detected using full activity space analysis
373 compared to residential location alone. Areas of core spatial intensity and significant spatial
374 effects based on activity space were generally larger, and sometimes included additional
375 geographic focal points, suggesting a notable portion of activity spaces may be located in areas
376 outside participants' home neighborhoods. A possible exception is group C, which had similar
377 exceedance areas in both analyses, suggesting activity spaces for these participants may
378 generally be located in closer proximity to place of residence. Relatively high unemployment in
379 group C and fewer work locations may have contributed to this observation. Our results show

380 that analyses based on residential location alone may not fully represent the spatial
381 characterization of hotspots.

382
383 Spatial analysis for infectious disease transmission involves an inherent assumption that the
384 locations analyzed are important with regard to transmission. Activity space analysis
385 incorporates important locations in the community where TB transmission may occur, and may
386 reduce exposure misclassification and improve the geographic characterization of transmission
387 chains⁴². This has implications for planning and evaluating targeted interventions⁴³. For example,
388 a recent TB modeling study found limited effectiveness of spatially targeted screening based on
389 proximity to household locations of people with incident TB in Peru⁴⁴. However, hotspots of TB
390 incidence based on household locations do not necessarily correspond with hotspots of
391 transmission^{43,44}. Activity space analysis may help address issues such as this in spatial analysis
392 for TB transmission.

393
394 Activity space analysis has an established history of use in fields such as social geography and
395 urban planning⁴⁵⁻⁴⁷. It fits naturally into the spatial epidemiology framework, which emphasizes
396 place and location-based health exposures^{23,48}. This approach acknowledges space as a social
397 determinant of health and helps incorporate the influence of social and physical environments on
398 health outcomes^{23,49}. However, there are relatively few examples of spatial analysis of activity
399 space in the TB literature. An early example that helped lay the foundation for activity space
400 analysis in TB research was a study to detect TB hotspots in Japan⁵⁰. The study incorporated
401 spatial and genomic data, though at a relatively low resolution (spatial data were aggregated at

402 the census tract level and genotype clustering identified using IS6110-based restriction fragment
403 length polymorphism (IS6110-RFLP) analysis)⁵⁰.

404

405 Our results are in line with studies of TB in the US²⁵ and South Africa²¹ that both noted
406 differences between ‘high-risk’ areas identified with density maps of activity spaces compared to
407 residential locations alone. These studies highlighted the potential importance of activity space
408 analysis, though neither study included genomic data.

409

410 Our results are also in line with a recent study in Peru that combined WGS and spatial data to
411 identify differences in activity spaces of genotypically related and unrelated cases and non-TB
412 controls²⁶. Notably, this study highlighted the potential to draw on methodology used in spatial
413 ecology, such as using UDs to model activity space, both at the individual and group level²⁶. The
414 approach taken in this study was to focus mainly on quantifying size (geographic area) and
415 amount of overlap among participants’ UDs, rather than detecting specific high-risk areas in the
416 community. Our study expanded on these methods by using a spatial point process model, which
417 allowed us to incorporate measures of uncertainty and detect potential hotspots by identifying
418 high-confidence areas of highest spatial intensity.

419

420 A limitation of our study is that incorporating activity space may have resulted in including
421 locations that are not relevant to transmission. Another limitation is that we did not include
422 specific measures of temporality, which is also an important element of transmission dynamics.

423

424 Another limitation of this study is that we did not examine potential contributing risk factors
425 driving the observed spatial patterns. Spatial variation is often a proxy for the influence of
426 unmeasured variables that may include sociodemographic, social, structural, or environmental
427 factors impacting risk^{36,51}. The spatial LGCP modeling approach can incorporate spatially-
428 referenced covariates⁵¹ (such as population-level sociodemographic characteristics or
429 environmental variables); however these data were not available for our analysis. We focused
430 primarily on identifying geographic areas of increased risk, which could potentially be targeted
431 for outreach such as active case finding. However, further analysis could incorporate additional
432 data or modeling techniques to assess potential risk factors.

433
434 Another limitation of this study is an unknown number of missing cases, activity space locations,
435 and WGS data that could potentially alter geographic characterization of genotypic groups.
436 Although the original study had relatively high enrollment (4,331/5,515 persons diagnosed
437 during the study period), not every person with TB was included, such as those diagnosed but not
438 enrolled and cases that were not detected. In addition, the use of location data obtained through
439 patient interviews is subject to recall bias and underreporting⁵². Other methods of obtaining
440 location data, such as prospective GPS tracking, have been suggested as potential alternatives²⁶.
441 However, locations visited during the infectious period prior to diagnosis and study enrollment
442 were of primary interest in this context⁵³. Further, a study comparing locations reported by
443 participants and locations captured via GPS loggers found that for three quarters of respondents,
444 over 70% of self-reported locations matched with the GPS data⁵⁴.

445

446 **Conclusion**

447 Integrated geospatial and genomic analysis of activity space may help identify potential high-risk
448 locations of sustained transmission in the community. Activity space analysis may improve the
449 geographic characterization of transmission ‘hotspots’ compared to analysis of residential
450 location alone. This could help with planning and mobilizing interventions to interrupt ongoing
451 transmission, and could provide a valuable tool for public health officials working to eliminate
452 TB among marginalized communities^{7,10}.

453

454 References

- 455 1. World Health Organization. Global Tuberculosis Report 2023. World Health Organization;
456 2023. Accessed March 3, 2024. <https://www.who.int/publications-detail-redirect/9789240083851>
- 457 2. Vesga JF, Hallett TB, Reid MJA, et al. Assessing tuberculosis control priorities in high-burden
458 settings: a modelling approach. *Lancet Glob Health*. 2019;7(5):e585-e595. doi:10.1016/S2214-
459 109X(19)30037-3
- 460 3. Auld SC, Shah NS, Cohen T, Martinson NA, Gandhi NR. Where is tuberculosis transmission
461 happening? Insights from the literature, new tools to study transmission and implications for the
462 elimination of tuberculosis. *Respirol Carlton Vic*. Published online June 5, 2018.
463 doi:10.1111/resp.13333
- 464 4. Shaweno D, Trauer JM, Doan TN, Denholm JT, McBryde ES. Geospatial clustering and
465 modelling provide policy guidance to distribute funding for active TB case finding in Ethiopia.
466 *Epidemics*. 2021;36:100470. doi:10.1016/j.epidem.2021.100470
- 467 5. Zetola NM, Moonan PK, Click E, et al. Population-based geospatial and molecular
468 epidemiologic study of tuberculosis transmission dynamics, Botswana, 2012–2016. *Emerg Infect*
469 *Dis*. 2021;27(3):835-844. doi:10.3201/eid2703.203840
- 470 6. Guthrie JL, Gardy JL. A brief primer on genomic epidemiology: lessons learned from
471 *Mycobacterium tuberculosis*. *Ann N Y Acad Sci*. 2017;1388(1):59-77.
472 doi:<https://doi.org/10.1111/nyas.13273>
- 473 7. Gardy JL, Loman NJ. Towards a genomics-informed, real-time, global pathogen surveillance
474 system. *Nat Rev Genet*. 2018;19(1):9-20. doi:10.1038/nrg.2017.88

- 475 8. Moonan PK, Ghosh S, Oeltmann JE, Kammerer JS, Cowan LS, Navin TR. Using Genotyping
476 and Geospatial Scanning to Estimate Recent Mycobacterium tuberculosis Transmission, United
477 States. *Emerg Infect Dis.* 2012;18(3):458-465. doi:10.3201/eid1803.111107
- 478 9. Shaweno D, Karmakar M, Alene KA, et al. Methods used in the spatial analysis of
479 tuberculosis epidemiology: a systematic review. *BMC Med.* 2018;16(1):193.
480 doi:10.1186/s12916-018-1178-4
- 481 10. Inzaule SC, Tessema SK, Kebede Y, Ogwell Ouma AE, Nkengasong JN. Genomic-informed
482 pathogen surveillance in Africa: opportunities and challenges. *Lancet Infect Dis.*
483 2021;21(9):e281-e289. doi:10.1016/S1473-3099(20)30939-7
- 484 11. Smith JP, Oeltmann JE, Hill AN, et al. Characterizing tuberculosis transmission dynamics in
485 high-burden urban and rural settings. *Sci Rep.* 2022;12(1):6780. doi:10.1038/s41598-022-10488-
486 2
- 487 12. Ribeiro FKC, Pan W, Bertolde A, et al. Genotypic and Spatial Analysis of Mycobacterium
488 tuberculosis Transmission in a High-Incidence Urban Setting. *Clin Infect Dis Off Publ Infect Dis*
489 *Soc Am.* 2015;61(5):758-766. doi:10.1093/cid/civ365
- 490 13. Zelner JL, Murray MB, Becerra MC, et al. Identifying Hotspots of Multidrug-Resistant
491 Tuberculosis Transmission Using Spatial and Molecular Genetic Data. *J Infect Dis.*
492 2016;213(2):287-294. doi:10.1093/infdis/jiv387
- 493 14. Li M, Lu L, Jiang Q, et al. Genotypic and spatial analysis of transmission dynamics of
494 tuberculosis in Shanghai, China: a 10-year prospective population-based surveillance study.
495 *Lancet Reg Health West Pac.* 2023;38:100833. doi:10.1016/j.lanwpc.2023.100833

- 496 15. Moonan PK, Oppong J, Sahbazian B, et al. What Is the Outcome of Targeted Tuberculosis
497 Screening Based on Universal Genotyping and Location? *Am J Respir Crit Care Med*.
498 2006;174(5):599-604. doi:10.1164/rccm.200512-1977OC
- 499 16. Shaweno D, Trauer JM, Doan TN, Denholm JT, McBryde ES. (Pre)Geospatial clustering and
500 modelling provide policy guidance to distribute funding for active TB case finding in Ethiopia.
501 *Epidemics*. Published online May 19, 2021:100470. doi:10.1016/j.epidem.2021.100470
- 502 17. Dowdy DW, Golub JE, Chaisson RE, Saraceni V. Heterogeneity in tuberculosis transmission
503 and the role of geographic hotspots in propagating epidemics. *Proc Natl Acad Sci U S A*.
504 2012;109(24):9557-9562. doi:10.1073/pnas.1203517109
- 505 18. Shrestha S, Reja M, Gomes I, et al. Quantifying geographic heterogeneity in TB incidence
506 and the potential impact of geographically targeted interventions in south and north city
507 corporations of Dhaka, Bangladesh: a model-based study. *Epidemiol Infect*. Published online
508 April 19, 2021:1-27. doi:10.1017/S0950268821000832
- 509 19. Reid MJA, Arinaminpathy N, Bloom A, et al. Building a tuberculosis-free world: The Lancet
510 Commission on tuberculosis. *The Lancet*. 2019;393(10178):1331-1384. doi:10.1016/S0140-
511 6736(19)30024-8
- 512 20. Nelson KN, Shah NS, Mathema B, et al. Spatial Patterns of Extensively Drug-Resistant
513 Tuberculosis Transmission in KwaZulu-Natal, South Africa. *J Infect Dis*. 2018;218(12):1964-
514 1973. doi:10.1093/infdis/jiy394
- 515 21. Peterson ML, Gandhi NR, Clennon J, et al. Extensively drug-resistant tuberculosis hotspots
516 and sociodemographic associations in Durban, South Africa. *Int J Tuberc Lung Dis Off J Int
517 Union Tuberc Lung Dis*. 2019;23(6):720-727. doi:10.5588/ijtld.18.0575

- 518 22. Yang C, Lu L, Warren JL, et al. Internal migration and transmission dynamics of tuberculosis
519 in Shanghai, China: an epidemiological, spatial, genomic analysis. *Lancet Infect Dis.*
520 2018;18(7):788-795. doi:10.1016/S1473-3099(18)30218-4
- 521 23. Kestens Y, Wasfi R, Naud A, Chaix B. “Contextualizing Context”: Reconciling
522 Environmental Exposures, Social Networks, and Location Preferences in Health Research. *Curr*
523 *Environ Health Rep.* 2017;4(1):51-60. doi:10.1007/s40572-017-0121-8
- 524 24. Matthews SA, Yang TC. Spatial Polygamy and Contextual Exposures (SPACES): Promoting
525 Activity Space Approaches in Research on Place and Health. *Am Behav Sci.* 2013;57(8):1057-
526 1081. doi:10.1177/0002764213487345
- 527 25. Worrell MC, Kramer M, Yamin A, Ray SM, Goswami ND. Use of Activity Space in a
528 Tuberculosis Outbreak: Bringing Homeless Persons Into Spatial Analyses. *Open Forum Infect*
529 *Dis.* 2017;4(1):ofw280. doi:10.1093/ofid/ofw280
- 530 26. Bui DP, Chandran SS, Oren E, et al. Community transmission of multidrug-resistant
531 tuberculosis is associated with activity space overlap in Lima, Peru. *BMC Infect Dis.*
532 2021;21(1):275. doi:10.1186/s12879-021-05953-8
- 533 27. Baker CR, Barilar I, de Araujo LS, et al. Use of High-Resolution Geospatial and Genomic
534 Data to Characterize Recent Tuberculosis Transmission, Botswana. *Emerg Infect Dis.*
535 2023;29(5):977-987. doi:10.3201/eid2905.220796
- 536 28. Zetola NM, Modongo C, Moonan PK, et al. Protocol for a population-based molecular
537 epidemiology study of tuberculosis transmission in a high HIV-burden setting: the Botswana
538 Kopanyo study. *BMJ Open.* 2016;6(5). doi:10.1136/bmjopen-2015-010046

- 539 29. ESRI. ArcGIS Desktop. Published online 2019.
- 540 30. Diggle PJ. Statistical Analysis of Spatial and Spatio-Temporal Point Patterns. 0 ed. Chapman
541 and Hall/CRC; 2013. doi:10.1201/b15326
- 542 31. Banerjee S, Carlin BP, Gelfand AE. Hierarchical Modeling and Analysis for Spatial Data.
543 CRC Press; 2014.
- 544 32. Watson J, Joy R, Tollit D, Thornton SJ, Auger-Méthé M. Estimating animal utilization
545 distributions from multiple data types: A joint spatiotemporal point process framework. Ann
546 Appl Stat. 2021;15(4). doi:10.1214/21-AOAS1472
- 547 33. Simpson D, Illian JB, Lindgren F, Sørbye SH, Rue H. Going off grid : computationally
548 efficient inference for log-Gaussian Cox processes. Published online March 2016.
549 doi:10.1093/biomet/asv064
- 550 34. Lindgren F, Rue H. Bayesian Spatial Modelling with R-INLA. J Stat Softw. 2015;63(19):1-
551 25.
- 552 35. Illian JB, Sørbye SH, Rue H. A toolbox for fitting complex spatial point process models
553 using integrated nested Laplace approximation (INLA). Ann Appl Stat. 2012;6(4):1499-1530.
554 doi:10.1214/11-AOAS530
- 555 36. Moraga P. Spatial Statistics for Data Science: Theory and Practice with R. Chapman &
556 Hall/CRC Data Science Series; 2023. Accessed November 5, 2023.
557 <https://www.paulamoraga.com/book-spatial/index.html>

- 558 37. Krainski, Gómez-Rubio, Bakka, et al. Advanced Spatial Modeling with Stochastic Partial
559 Differential Equations Using R and INLA.; 2019. Accessed November 5, 2023.
560 <https://becarioprecario.bitbucket.io/spde-gitbook/index.html>
- 561 38. Gómez-Rubio V. Bayesian Inference with INLA.; 2021. Accessed November 7, 2023.
562 <http://becarioprecario.bitbucket.io/inla-gitbook/index.html>
- 563 39. Rue H, Martino S, Chopin N. Approximate Bayesian inference for latent Gaussian models by
564 using integrated nested Laplace approximations. *J R Stat Soc Ser B Stat Methodol.*
565 2009;71(2):319-392. doi:10.1111/j.1467-9868.2008.00700.x
- 566 40. Bachl FE, Lindgren F, Borchers DL, Illian JB. inlabru: an R package for Bayesian spatial
567 modelling from ecological survey data. *Methods Ecol Evol.* 2019;10(6):760-766.
568 doi:10.1111/2041-210X.13168
- 569 41. Palmí-Perales F, Gómez-Rubio V, López-Abente G, Ramis R, Sanz-Anquela JM, Fernández-
570 Navarro P. Approximate Bayesian inference for multivariate point pattern analysis in disease
571 mapping. *Biom J.* 2021;63(3):632-649. doi:10.1002/bimj.201900396
- 572 42. Keshavjee S, Dowdy D, Swaminathan S. Stopping the body count: a comprehensive
573 approach to move towards zero tuberculosis deaths. *The Lancet.* 2015;386(10010):e46-e47.
574 doi:10.1016/S0140-6736(15)00320-7
- 575 43. Huang CC, Trevisi L, Becerra MC, et al. Spatial scale of tuberculosis transmission in Lima,
576 Peru. *Proc Natl Acad Sci U S A.* 2022;119(45):e2207022119. doi:10.1073/pnas.2207022119

- 577 44. Havumaki J, Warren JL, Zelner J, et al. Spatially-targeted tuberculosis screening has limited
578 impact beyond household contact tracing in Lima, Peru: A model-based analysis. PLOS ONE.
579 2023;18(10):e0293519. doi:10.1371/journal.pone.0293519
- 580 45. Browning CR, Soller B. Moving Beyond Neighborhood: Activity Spaces and Ecological
581 Networks As Contexts for Youth Development. Cityscape Wash DC. 2014;16(1):165-196.
- 582 46. Horton FE, Reynolds DR. Effects of Urban Spatial Structure on Individual Behavior. Econ
583 Geogr. 1971;47(1):36. doi:10.2307/143224
- 584 47. Xi W, Calder CA, Browning CR. Beyond Activity Space: Detecting Communities in
585 Ecological Networks. Ann Am Assoc Geogr. 2020;110(6):1787-1806.
586 doi:10.1080/24694452.2020.1715779
- 587 48. Elliott P, Wartenberg D. Spatial Epidemiology: Current Approaches and Future Challenges.
588 Environ Health Perspect. 2004;112(9):998-1006. doi:10.1289/ehp.6735
- 589 49. Ortblad KF, Salomon JA, Bärnighausen T, Atun R. Stopping tuberculosis: a biosocial model
590 for sustainable development. Lancet Lond Engl. 2015;386(10010):2354-2362.
591 doi:10.1016/S0140-6736(15)00324-4
- 592 50. Izumi K, Ohkado A, Uchimura K, et al. Detection of Tuberculosis Infection Hotspots Using
593 Activity Spaces Based Spatial Approach in an Urban Tokyo, from 2003 to 2011. PLoS ONE.
594 2015;10(9). doi:10.1371/journal.pone.0138831
- 595 51. Diggle PJ, Moraga P, Rowlingson B, Taylor BM. Spatial and Spatio-Temporal Log-Gaussian
596 Cox Processes: Extending the Geostatistical Paradigm. Stat Sci. 2013;28(4). doi:10.1214/13-
597 STS441

- 598 52. Surie D, Fane O, Finlay A, et al. Molecular, Spatial, and Field Epidemiology Suggesting TB
599 Transmission in Community, Not Hospital, Gaborone, Botswana. *Emerg Infect Dis.*
600 2017;23(3):487-490. doi:10.3201/eid2303.161183
- 601 53. Bui DP, Oren E, Roe DJ, et al. A Case-Control Study to Identify Community Venues
602 Associated with Genetically-clustered, Multidrug-resistant Tuberculosis Disease in Lima, Peru.
603 *Clin Infect Dis.* 2019;68(9):1547-1555. doi:10.1093/cid/ciy746
- 604 54. Kestens Y, Thierry B, Shareck M, Steinmetz-Wood M, Chaix B. Integrating activity spaces in
605 health research: Comparing the VERITAS activity space questionnaire with 7-day GPS tracking
606 and prompted recall. *Spat Spatio-Temporal Epidemiol.* 2018;25:1-9.
607 doi:10.1016/j.sste.2017.12.003
- 608